UDC 004.855.5(045)
DOI:10.18372/1990-5548.84.20193

[1]V. M. Sineglazov,
[2]V. O. Fedirko,
[3]V. V. Shust,
[4]A. V. Sheruda,
[5]M. V. Shevchenko

DIAGNOSIS OF VESTIBULAR SCHWANNOMA BASED ON INTELLIGENT MRI IMAGE PROCESSING

[1,5]Aviation Computer-Integrated Complexes Department, Faculty of Air Navigation Electronics and Telecommunications, State University "Kyiv Aviation Institute", Kyiv, Ukraine
[2,3]Romodanov Institute of Neurosurgery NAMS of Ukraine, Kyiv, Ukraine
[4]Faculty of Informatics and Computer Science, National Technical University of Ukraine "Ihor Sikorsky Kyiv Polytechnic Institute," Kyiv, Ukraine
E-mails: [1]svm@nau.edu.ua ORCID 0000-0002-3297-9060,
[2]fedirkovol@gmail.com ORCID 0000-0002-0411-6161
[3]vasulshust97@gmail.com ORCID 0000-0002-0459-9888
[4]sheruda.andrew@lll.kpi.ua, [5]maksymshevchenko01@gmail.com

***Abstract*—*The study identified the main clinical and diagnostic features of the disease, reviewed modern diagnostic methods for schwannoma, including magnetic resonance imaging and computed tomography, as well as the role of clinical examination, history and laboratory tests, analyzed available open data and proposed the concept of combining medical images with molecular indicators to build more effective diagnostic models based on semantic segmentation. Diagnostic and prognostic biomarkers were summarized, including TNF-α, CD68, CD163, IL-6, CCR2 and others, which may increase the accuracy of predicting the course of the disease.*

Keywords—Vestibular schwannoma; diagnostic and prognostic biomarkers; MRI images; convolutional neural network; Transformers; semantic segmentation.

I. INTRODUCTION

Vestibular schwannoma (VS), also known as acoustic neuroma, is a benign tumor arising from Schwann cells of the vestibular-auditory nerve. Despite its slow growth in the most cases the tumor can cause significant neurological impairment due to compression of adjacent structures, which requires timely and accurate diagnosis. Currently, magnetic resonance imaging (MRI), particularly with contrast enhancement, remains the gold standard for VS diagnosis. However, modern imaging methods have several limitations: they require the involvement of highly qualified specialists, are subject to subjective interpretation, and are poorly adapted to automated prediction of tumor dynamics. In addition, traditional approaches rarely consider biomolecular markers that may reflect inflammatory processes or the potential for rapid tumor growth.

Thus, there is a clear lack of comprehensive diagnostic systems capable of integrating visual and molecular data to improve the accuracy and prognostic value of disease detection. Furthermore, the shortage of qualified medical personnel and the overload of healthcare institutions hinder timely detection of tumors, which negatively affects patient outcomes.

This study aims to address these challenges by applying artificial intelligence methods. The main objective is to develop an intelligent model that uses MRI data for semantic segmentation of the tumor and prediction of its behavior. This will enable the creation of more accurate and reproducible diagnostic systems that can support clinicians in the decision-making process.

II. SCHWANNOMAS AND THEIR SIGNS

Schwannomas usually grow slowly but steadily. In most cases, as shown in Fig. 1, they are unilateral and solitary [1], but in patients with neurofibromatosis type 2 (NF2), they can be bilateral and have a more aggressive course.

Although this tumor is histologically benign, its location in a limited intracranial space leads to compression of surrounding structures, causing hearing impairment, balance impairment, and in advanced cases, brainstem compression and hydrocephalus.

Today, the problem of timely diagnosis and effective treatment of brain tumors, including

vestibular schwannoma, remains highly relevant due to the often asymptomatic course at early stages and limited access to specialized diagnostic technologies and experienced medical professionals in some regions.

Last time an increase in the number of cases of this tumor mentioned due to wider MRI application and revealing VS in cases with "silent" signs. At the same time, the shortage of medical workers and the workload of health care institutions complicate the availability of quality medical services, lack of the onconvigilance which often leads to late detection of tumors and a worsening prognosis for patients. Early diagnosis let remove tumor with saving cochlear and facial nerves without complications.

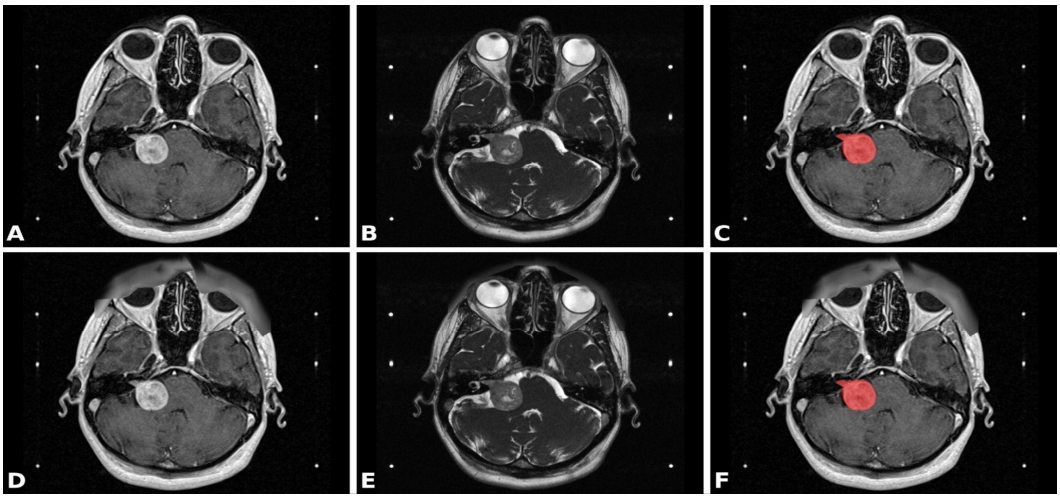

Fig. 1. Illustrative example of a dataset of a patient with a right vestibular schwannoma (VS): (a) Contrast-enhanced T1-weighted MRI (ceT1); (b) High-resolution T2-weighted MRI (hrT2); (c) ceT1 MRI with annotated segmentation of the VS; (d) – (f) corresponding images after facial features are obscured. The six white dots in each image are the reference points of the indicator field of the Lexel stereotaxic system used for image co-registration [1]

III. Clinical and Diagnostic Features

The main symptoms of vestibular schwannoma are associated with the gradual damage to the auditory and vestibular apparatus:

- hearing loss (unilateral or bilateral);
- tinnitus;
- balance disorders and dizziness;
- facial nerve paresis with tumor growth;
- headache, nausea, impaired coordination in case of a large tumor.

Diagnosis is based primarily on magnetic resonance imaging with contrast – the gold standard for imaging this pathology. On MRI, schwannoma usually appears as a clearly delineated iso- or hypointense formation on T1-weighted images with intense contrast enhancement, and as hyperintense on T2-weighted images. In some cases, CT is also used to assess the condition of the bone structures of the temporal bone pyramid and the internal auditory canal.

IV. Tumor Markers and Biomarkers in Schwannoma

We have a certain number of basic biomarkers, tumor markers and their reference values in Table I.

Table I. A Variety of Tumor Markers, Biomarkers, their Significance in Schwannoma from Different Sources

Marker	Material	Value / Correlation	Source
TNF‑α (Plasma)	Blood	13.05 ± 2.29 pg/mL vs. 5.97 ± 1.20 in controls ($p < 0.05$)	[2] PMC Immunoprofiling
TNF‑α (Perilymph)	Perilymph	20.59 ± 1.62 pg/mL vs. 3.14 ± 2.57 in controls ($p < 0.001$)	[2] PMC Immunoprofiling
TWEAK (Perilymph)	Perilymph	19.25 ± 6.56 pg/mL; approximately 3.3 times higher than in blood ($p < 0.0001$)	[2] PMC Immunoprofiling
CD68	IHC/RT‑qPCR	$r = 0.28$ correlation with tumor volume ($p < 0.0001$)	[3] PMC correlation study

Ending of Table I

CD163	IHC/RT‑qPCR	$r = 0.19$ correlation with volume ($p = 0.02$); higher expression in fast-growing tumors	[3] PMC correlation study
IL‑1β	scRNAseq/IHC	Strong regional expression, correlates with tumor volume	[4] Nature scRNA-seq
IL‑6	scRNAseq/IHC	Moderate expression, correlates with tumor volume	[4] Nature scRNA-seq
CCR2	IHC	Significantly elevated in NF2-associated tumors ($p < 0.0001$)	[4] Frontiers Oncology
CD14	scRNAseq	Strong correlation with tumor volume ($\rho = 0.71$, $p = 0.027$)	[4] Nature scRNA-seq
PD‑L1	IHC	Positive association with tumor growth in presence of CD163 ($p < 0.05$)	[5] ResearchGate VS volume study
CFHR2	Mass spectrometry	Elevated in perilymph of patients with severe hearing loss	[6] Scientific Reports proteome

Each tumor marker and biomarker found in vestibular schwannoma has its own explanation:

1) *TNF-α* (Tumor Necrosis Factor α. Inflammatory Biomarker) is a potent pro-inflammatory cytokine involved in the development of inflammation, apoptosis, and regulation of the immune response. Elevated levels of TNF-α in the blood and perilymph of schwannoma patients indicate active inflammation that may contribute to auditory nerve damage and tumor progression. Its high concentrations correlate with hearing loss.

2) *TWEAK* (TNF-like Weak Inducer of Apoptosis. Inflammatory Biomarker) is a cytokine related to the TNF family that affects apoptosis, proliferation, and angiogenesis. In schwannoma patients, TWEAK is found at high concentrations in the perilymph, indicating its role in inner ear damage and possible stimulation of tumor growth.

3) *CD68* (Immune biomarker) is a marker of macrophages, cells responsible for phagocytosis and immune response. High levels of CD68 in schwannoma tissue indicate active immune infiltration. Its expression correlates with tumor size, indicating the involvement of macrophages in its growth.

4) *CD163* (Immune biomarker) is a marker of M2 macrophages (alternatively activated), associated with immune tolerance and tissue repair. Increased expression of CD163 is associated with rapid schwannoma growth, suppression of the immune response and possible tumor progression.

5) *IL-1β* (Interleukin-1 beta. Inflammatory biomarker) is a pro-inflammatory cytokine that stimulates the immune response, T-cell activation and the production of other mediators. Strong expression of IL-1β in schwannoma tissues suggests an inflammatory tumor microenvironment that may promote tumor growth and cause symptoms (e.g., pain or swelling).

6) *IL-6* (Inflammatory biomarker) is a pro-inflammatory and anti-inflammatory cytokine involved in tumor growth and angiogenesis. Its presence indicates the maintenance of chronic inflammation, which likely contributes to tumor expansion and neurodegeneration.

7) *CCR2* (Immune biomarker) is a receptor for monocyte chemoattractants. High expression of CCR2 in schwannoma is associated with monocyte and macrophage infiltration. It is often elevated in cases of neurofibromatosis type 2 (NF2), which may indicate a more aggressive tumor.

8) *CD14* (Immune biomarker) is a receptor associated with innate immunity that recognizes bacterial components. In schwannomas, it is expressed on macrophages; its expression may correlate with tumor growth rate, indicating activation of the innate immune response.

9) *PD-L1* (Programmed Death-Ligand 1. Tumor marker/immune marker) is an immune inhibitor that suppresses T-cell activation. Its increased expression in schwannoma indicates immune evasion of the tumor, i.e. its ability to avoid destruction by the immune system. PD-L1 is particularly active in tumors with increased CD163.

10) *CFHR2* (Complement Factor H-Related Protein 2) is a protein involved in the regulation of the complement system. High levels of CFHR2 in the perilymph are associated with severe hearing impairment in schwannoma patients. Its role is to modify the inflammatory state.

V. Overview of Modern Approaches to the Diagnosis of Schwannoma

Based on the work from scientific sources, Table II summarizes current approaches to the diagnosis of vestibular schwannoma, the proposed approach for each source, and the disadvantages of a particular approach.

A. Primary diagnosis: examination, history and screening

Diagnosis begins with a clinical examination of the patient by an otoneurologist or neurologist, who assesses the neurological status, coordination of movements, facial sensitivity, hearing and balance. Unilateral hearing loss, tinnitus, balance disorders, and sometimes mild facial nerve paresis are often detected.

The history is important: the doctor finds out the time of onset of symptoms, their nature, progression, the presence of injuries, hereditary diseases, in particular neurofibromatosis type II. It is also important to clarify whether the patient has systemic or vascular pathologies that can mask the symptoms of schwannoma.

TABLE II. MODERN APPROACHES TO THE DIAGNOSIS OF VESTIBULAR SCHWANNOMA

No.	Source	Proposed Approach	Limitations of Approach
1	Lee et al., 2024, Scientific Reports	Schwannoma segmentation on MRI using U-Net	Loss of context between slices, reduced accuracy with complex tumor geometry
2	Lee et al., 2021, Scientific Reports	Semi-automatic MRI annotation with physician involvement	Dependence on human factor, scalability challenges
3	Chen et al., 2024, arXiv	Application of transformers for MRI analysis	High computational resources, limited interpretability, dependence on large datasets
4	George-Jones et al., 2021, ResearchGate	Analysis of tumor texture and shape on MRI	Sensitivity to noise, instability of texture features with scan parameter changes
5	Zhou et al., 2022, PubMed	Schwannoma classification using machine learning	Limited clinical validation, possible overfitting, poor generalization
6	Lu et al., 2022, PMC	3D segmentation based on T2 MRI	High computational demands, sensitivity to image quality
7	Yüksel et al., 2020, Journal of Surgery and Medicine	Conventional MRI evaluation using FLAIR and SWI sequences	Not all clinics use required sequences, limited generalizability of case
8	Strohl et al., 2020, Journal of the American Academy	Combined diagnostics: CT, MRI, audiometry	Interpretation complexity with comorbidities, need for multidisciplinary approach
9	Park et al., 2014, Journal of the Korean Society of Radiology	Contrast-enhanced MRI + CT angiography	Angiography is invasive, limited routine use
10	Ravindra et al., 2012, Surgical Neurology International	Dynamic MRI monitoring over several years	Atypical case, inability to standardize approach without active intervention
11	Ali & Syed, 2023, TCIA – Vestibular-Schwannoma-SEG	Public annotated dataset for model training	Limited universality, possible legal restrictions, lack of clinical adaptation

In the presence of symptoms, audiometric tests (pure tone audiometry, impedancemetry) are performed, which reveal sensorineural hearing loss – typical of schwannoma. Additionally, vestibular tests may be prescribed, for example, videonystagmography or the Romberg test. Instrumental detection methods.

B. Magnetic resonance imaging (MRI)

Contrast-enhanced MRI is the "gold standard" for the diagnosis of schwannoma. This method allows the detection of even very small tumors (less than 2 mm in diameter), especially in the internal auditory canal.

Recommended MRI parameters for the detection of schwannoma:

- *mode:* T1 and T2-weighted images;
- *contrast:* gadolinium (0.1 mmol/kg);
- *slice thickness:* 1–2 mm;
- *scan plan:* axial and coronal, oriented to the cerebellopontine angle;
- *special sequences:* 3D-CISS or FIESTA for detailing the internal auditory canal.

C. Computed tomography (CT)

Computed tomography is used less frequently, mainly to evaluate bony structures. It helps to visualize the dilation of the internal auditory canal, which is an indirect sign of schwannoma.

Recommended CT parameters:

- *slice thickness:* 0.6–1 mm;
- *mode:* high-resolution CT (HRCT);
- *orientation:* axial and coronal projections.

D. Clinical examples

A review of clinical cases reported in the scientific literature [14], [15], [24], [25], presented in Table III, demonstrates the variability in the course of vestibular schwannoma. Some patients present with typical symptoms (hearing loss, tinnitus, balance disorders), while others present with unusual features such as the Tullio effect or variable tumor size.

TABLE III. REVIEW OF CLINICAL CASES

No.	Source	Age, Sex	Complaints	Examinations	Case Features
[14]	Journal of Surgery and Medicine (2020)	53 y.o., male	Tinnitus, ataxia	MRI, blood tests, clinical exam	Detected siderosis; schwannoma complicated by hemorrhages
[15]	J. Am. Acad. Audiol. (2020)	58 y.o., female	Tullio phenomenon, tinnitus	Audiometry, CT, MRI	Concurrent defect of the semicircular canal
[24]	J. Korean Soc. Radiol. (2014)	52 y.o., female	Headache, tinnitus	Contrast-enhanced MRI, CT angiography	Hypervascular tumor
[25]	Surg. Neurol. Int. (2012)	~60 y.o., N/A	Hearing loss	Dynamic MRI, audiogram	Tumor size changes without treatment

Patient 1:

Description: This article presents a rare clinical case of vestibular schwannoma complicated by superficial siderosis caused by chronic subarachnoid hemorrhage.

Patient: 53-year-old male with a long history of hearing loss, ataxia, and tinnitus.

Examination: General examination, blood tests (normal), neurological deficit (unsteady gait, sensorineural deafness), contrast-enhanced brain MRI showed hyperintense signals on T2-weighted images in the cerebellopontine angle and hemosiderin deposits in the meninges.

Patient 2:

Description: This case describes a 58-year-old female patient with a rare combination of superior semicircular canal defect syndrome and vestibular schwannoma.

History: vertigo with sounds (Tullio effect), feeling of "falling", tinnitus.

Examination: videooculography, audiogram (hearing loss at high frequencies), CT of temporal bones (confirmation of canal defect), MRI with gadolinium revealed a small rounded mass in the internal auditory canal.

Patient 3:

Description: We present a clinical case of a 52-year-old female patient with a hypervascular schwannoma, which was discovered during examination for headache.

History: slight tinnitus, headache without vestibular symptoms.

Examination and testing: physical examination without abnormalities, contrast MRI revealed a mass with intense vascular enhancement, CT angiography confirmed the hypervascularity of the tumor.

Patient 4:

Description: This case report describes a patient with an unstable schwannoma that had regressed from decreasing to increasing without treatment.

History: gradual unilateral hearing loss over a 3-year period.

Examination: audiometry, physical examination (neurologically unremarkable), MRI (several times over 3 years) – first tumor reduction, then growth was observed.

In patient 1, MRI with contrast demonstrated a distinct, lobular, contrast-enhancing lesion in the left cerebellar pontine region extending into the intracanal segment of the left internal auditory canal. The mass lesion measured 23x18 mm and displaced and compressed the pons and fourth ventricle (Fig. 2).

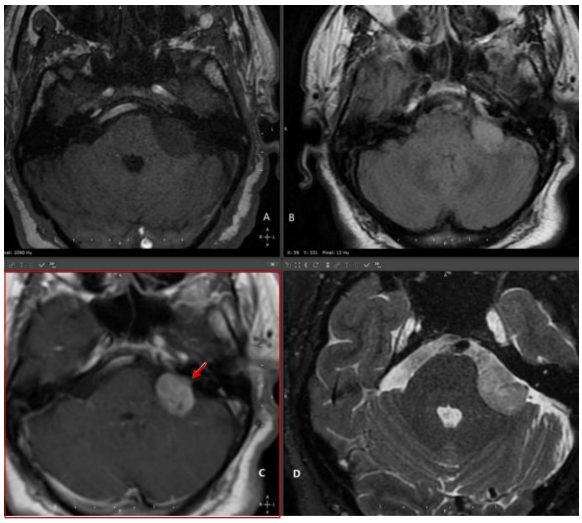

Fig. 2. Initial MRI scan. Axial T1A (a), FLAIR (b), post-contrast T1A (c), and TSE T2A (d). Extension into the intracanal segment of the left internal auditory canal (red arrow) [14]

VI. USING ARTIFICIAL INTELLIGENCE TO DETECT SCHWANNOMA

Intelligent processing of images obtained using computed tomography (CT) and magnetic resonance imaging (MRI) is one of the key areas of modern medical informatics. With the growth of medical data[12] – [15] and the need for high-precision diagnostics, artificial intelligence (AI) methods are becoming increasingly relevant, capable of automating image analysis and providing more accurate, fast and objective interpretation of results.

A. Processing of CT and MRI images in modern diagnostics

Images obtained using CT and MRI contain a large amount of structural information about the tissues of the body. However, the effective use of these data requires highly qualified personnel, significant time for analysis and the availability of specific knowledge. In this regard, automated processing of medical images based on machine learning and deep learning is a promising solution for improving the accuracy and efficiency of medical diagnostics.

In the case of schwannoma diagnosis, MRI is the main imaging modality because it provides high soft tissue contrast. The main steps of image processing are pre-normalization, smoothing, segmentation of pathological areas, feature extraction, and classification. Algorithms based on convolutional neural networks (CNN) and, more recently, transformer architectures are used for automatic tumor detection and segmentation.

B. Convolutional Neural Networks in MRI Processing

Convolutional neural networks (CNNs) are a leading approach to medical image processing due to their ability to automatically detect local and spatial features in an image. CNNs can effectively segment vestibular schwannoma, separating it from surrounding tissues. In particular, a study by Lee et al. demonstrated the possibility of accurately measuring changes in tumor volume on a series of MRI images after radiosurgery using specialized deep neural networks [16] – [19].

Convolutional neural networks models such as U-Net (Fig. 3), ResUNet or V-Net, adapted to the three-dimensional nature of medical images, especially MRI, allow for automatic detection of tumor boundaries, reducing the need for manual intervention by the physician.

C. Transformers in Medical Image Processing

Transformers, originally developed for natural language processing, have also been successfully applied to medical image segmentation. Architectures such as the Vision Transformer (ViT), Swin Transformer, and SegFormer (Fig. 4.) have demonstrated promising results.

Compared to CNNs, transformers better capture the global context of the image, which can be useful for segmenting tumors with complex shapes and sizes. In a recent study (Chen Y. et al., 2024), presented on arXiv, the Time Conditioned Neural Fields method was developed, which integrates a time factor into the transformer model to predict schwannoma growth based on a series of MRI images [20] – [23].

VII. PROBLEM STATEMENT AND METRICS USED

A. Problem statement

This study addresses the problem of semantic segmentation of a sequence of single-channel medical images of vestibular schwannoma, denoted as

$$X = \{x_t \mid x_t \in \mathbb{R}^{H \times W}\}, t = 1,\ldots,T,$$

where x_t represents the MRI scan of the schwannoma at time step t, with spatial resolution $H \times W$; T is the number of slices (or time frames) in the sequence.

For each image x_t, there exists a corresponding binary segmentation map $y_t \in 0,1^{H \times W}$, where pixel values indicate class membership:

– $y_{t,j,k} = 0$ is the background class,

– $y_{t,j,k} = 1$ is the schwannoma region.

The objective is to learn a segmentation function parameterized by a set of parameters θ, that maps the input sequence X to a set of predicted segmentation such that they closely approximate the ground-truth labels under a given similarity measure.

Images were passed as input to the segmentation models.

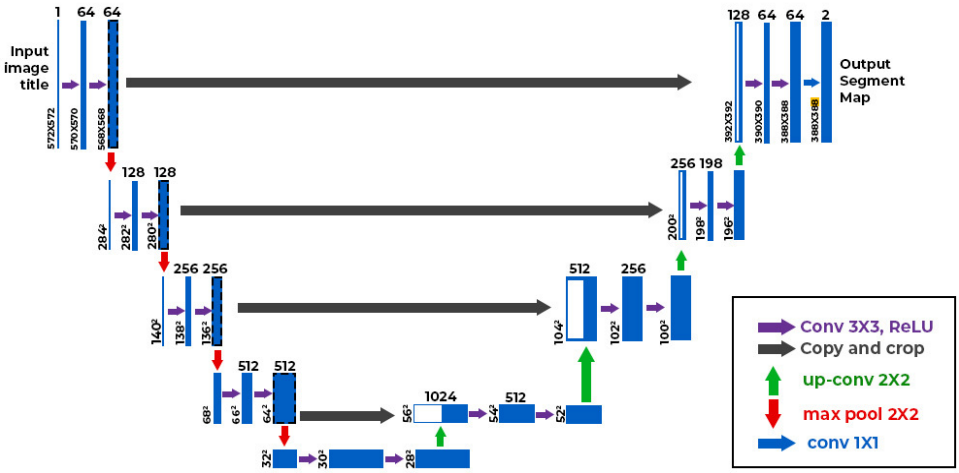

Fig. 3. U-net architecture

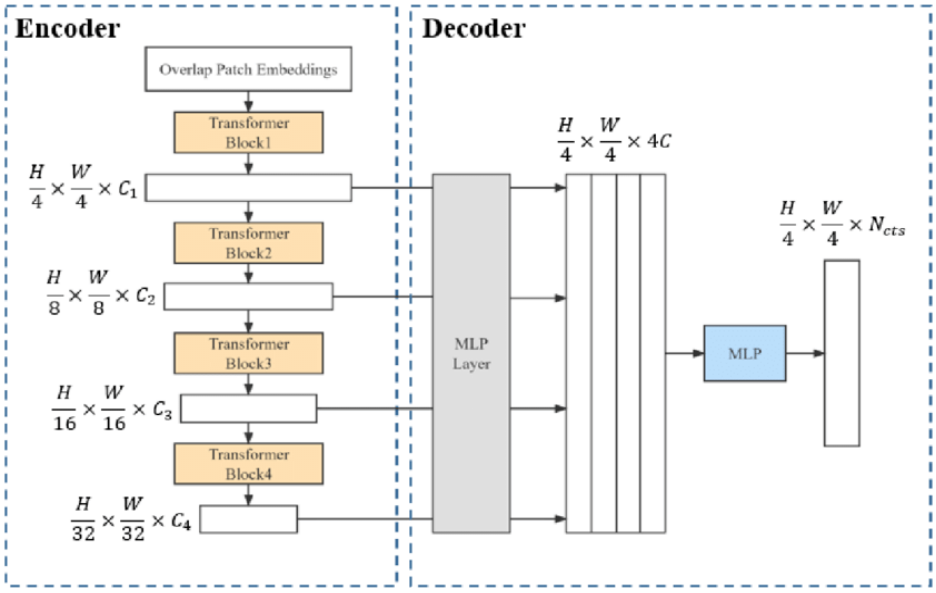

Fig. 4. SegFormer architecture

B. Metrics

In the context of semantic segmentation, evaluation metrics are computed by comparing predicted segmentation masks $\hat{y} \in 0,1^{H \times W}$ with corresponding ground-truth labels $y \in 0,1^{H \times W}$, on a per-pixel basis. For binary segmentation (e.g., "background" vs "schwannoma"), the segmentation task can be interpreted as a large-scale binary classification problem at the pixel level, with the following quantities:

- *true positive (TP):* the number of pixels correctly predicted as belonging to the target class (e.g., schwannoma);
- *false positive (FP):* the number of background pixels incorrectly predicted as tumor;
- *false negative (FN):* the number of tumor pixels incorrectly predicted as background.

Based on these, we define the following evaluation metrics.

1) Intersection over Union (IoU)

IoU, also known as the Jaccard Index, measures the overlap between the predicted and ground-truth segmentation masks, normalized by their union:

$$\text{IoU} = \frac{\text{TP}}{\text{TP} + \text{FP} + \text{FN}}.$$

This metric reflects the quality of the predicted segmentation region, penalizing both over- and under-segmentation. It is widely used in segmentation benchmarks due to its intuitive interpretation.

2) Precision

Precision quantifies the proportion of predicted tumor pixels that are truly part of the tumor:

$$\text{Precision} = \frac{\text{TP}}{(\text{TP}+\text{FP})}.$$

High precision indicates that few background pixels are misclassified as tumor (low false positive rate), which is important in avoiding over-segmentation.

3) Recall

Recall measures the proportion of actual tumor pixels that have been correctly identified by the model:

$$\text{Recall} = \frac{\text{TP}}{(\text{TP}+\text{FN})}.$$

This metric is particularly important in medical segmentation tasks, where missing a part of the lesion can lead to clinical underestimation of the condition.

4) F1-score:

The F1-score is the harmonic mean of precision and recall:

$$F1 = 2 \times \frac{(\text{Precision} \times \text{Recall})}{(\text{Precision}+\text{Recall})}.$$

$F1$ balances both false positives and false negatives and is often used when both types of errors are considered equally critical.

5) F2-score:

The $F2$-score is a generalization of the $F1$-score that weights recall more heavily than precision:

$$F2 = \frac{5 \times (\text{Precision} \times \text{Recall})}{(4 \times \text{Precision}+\text{Recall})}.$$

This metric is useful in clinical applications where false negatives (i.e., missed tumor regions) are more harmful than false positives.

VIII. RESULTS

The dataset used in this study consisted of a total of 1,527 MRI images collected from 93 patients. Among these, 780 frames contained manually annotated regions of vestibular schwannoma, while the remaining frames represented background without tumor presence.

The quantitative evaluation of segmentation performance across six state-of-the-art deep learning architectures is presented in Table IV. The models were assessed using standard semantic segmentation metrics, including Intersection over Union (IoU), Precision, Recall, F1-score, and F2-score.

TABLE IV. SEGMENTATION PERFORMANCE METRICS FOR DIFFERENT MODELS

Model	IoU	Precision	Recall	F1-score	F2-score
U-Net	0.783	0.802	0.768	0.785	0.774
U-Net++	0.794	0.812	0.779	0.795	0.785
DeepLabV3+	0.811	0.827	0.804	0.815	0.809
Attention U-Net	0.821	0.836	0.817	0.826	0.821
SegFormer	0.837	0.849	0.831	0.840	0.835
nnU-Net	0.858	0.865	0.852	0.858	0.855

The baseline **U-Net** model achieved an IoU of 0.783, with an $F1$-score of 0.785 and an $F2$-score of 0.774, reflecting its solid ability to localize the tumor but with limited robustness to false negatives. Its improved variant, **U-Net++**, yielded slightly higher performance (IoU = 0.794), indicating that the added nested skip connections enhanced feature representation and refinement.

DeepLabV3+ showed further improvements, with an IoU of 0.811 and $F1$-score of 0.815, confirming its effectiveness in capturing multiscale context via atrous spatial pyramid pooling. **Attention U-Net** demonstrated notable gains in recall (0.817) and $F2$-score (0.821), suggesting that attention mechanisms improve the model's sensitivity to the tumor region, which is crucial in clinical applications where false negatives must be minimized.

The transformer-based **TransUNet** outperformed convolutional models, achieving an IoU of 0.837 and F1-score of 0.840. This result underlines the capacity of hybrid architectures to model long-range dependencies in medical image data. The best overall performance was observed for **nnU-Net**, which obtained the highest IoU (0.858), precision (0.865), and $F1$/$F2$ scores (0.858 and 0.855, respectively). This demonstrates the strength of auto-configuring frameworks that optimize preprocessing, architecture, and training pipelines for the specific dataset characteristics.

IX. CONCLUSION

This study defined the key clinical and diagnostic features of vestibular schwannoma, analyzed available open datasets, to develop more effective diagnostic models.

Using a dataset of 1,527 MRI images from 93 patients, with 780 frames containing annotated tumor regions, several state-of-the-art deep learning architectures were developed and evaluated for automatic semantic segmentation of vestibular schwannoma. Advanced models, particularly transformer-based networks and the nnU-Net framework, demonstrated superior performance in accurately delineating tumor boundaries, as reflected in improved IoU, *F*1, and *F*2 metrics.

The proposed segmentation approaches have the potential to assist clinicians in precise tumor delineation, volumetric assessment, and growth monitoring, thus supporting timely surgical decision-making and personalized treatment planning.

Future research will focus on expanding multimodal datasets by incorporating molecular markers alongside imaging data, as well as leveraging temporal information to enhance the robustness and clinical relevance of predictive diagnostic models.

REFERENCES

[1] S. Ali, & A. M. Syed, "Vestibular-Schwannoma-SEG: Annotated MRI Dataset for Tumor Segmentation," *The Cancer Imaging Archive (TCIA)*, 2023. https://www.cancerimagingarchive.net/collection/vestibular-schwannoma-seg/

[2] R. C. Thompson, S. M. Stevens,, D. C. Miller, et al. "Proteomic analysis identifies fluid biomarkers associated with vestibular schwannoma–associated hearing loss," *Frontiers in Neurology*, 15, 11807327, 2024. https://www.ncbi.nlm.nih.gov/pmc/articles/PMC11807327/

[3] F. J. Gomez, D. J. Lee, & J. C. Wu, "Single-cell transcriptomic analysis reveals immune landscape of sporadic and NF2-related vestibular schwannomas," *Neuro-Oncology Advances*, 4(1), vdac127, 2022. https://www.ncbi.nlm.nih.gov/pmc/articles/PMC9496830/

[4] R. H. Jones, D. Patel, & L. M. Smith, "The tumour microenvironment in vestibular schwannoma: Immunological and molecular perspectives," *British Journal of Cancer*, 130, 842–853, 2024. https://www.nature.com/articles/s41416-024-02646-2

[5] L. Leisz, R. Fahlbusch, & M. Buchfelder, "Vestibular schwannoma volume and tumor growth correlates with macrophage marker expression," *Scientific Reports*, 12, Article 14799, 2022. https://www.researchgate.net/publication/363485341_Vestibular_Schwannoma_Volume_and_Tumor_Growth_Correlates_with_Macrophage_Marker_Expression_Academic_Editors_Yasin_Temel_and. https://doi.org/10.3390/cancers14184429

[6] Stankovic Lab – Stanford University School of Medicine. (n.d.). *Research overview: Translational studies on hearing loss and vestibular schwannoma*. Retrieved from. https://med.stanford.edu/stankovic-lab/research.html

[7] S. M. Heman-Ackah, R. Blue, S. P. Gubbels, A. D. Sweeney, and M. L. Carlson, "Machine learning-based prediction of facial nerve outcomes following vestibular schwannoma microsurgery," *Scientific Reports*, vol. 14, Article number: 6541, 2024. https://doi.org/10.1038/s41598-024-63161-1

[8] C. C. Lee, W. H. Lee, C. H. Wu, et al., "Applying artificial intelligence to longitudinal imaging analysis of vestibular schwannoma following radiosurgery," *Scientific Reports*, vol. 11, Article number: 3300, 2021. https://doi.org/10.1038/s41598-021-82665-8

[9] Y. Chen, J. M. Wolterink, O. Neve, et al. "DeepGrowth: Vestibular schwannoma growth prediction from longitudinal MRI by time conditioned neural fields," *arXiv preprint*, 2024. arXiv:2404.02614. – URL: https://arxiv.org/abs/2404.02614

[10] N. A. George-Jones, K. Wang, J. Wang, and J. B. Hunter, "Prediction of vestibular schwannoma enlargement after radiosurgery using tumor shape and MRI texture features," *ResearchGate*, 2021. URL: https://www.researchgate.net/publication/347850268

[11] N. A. George-Jones, K. Wang, J. Wang, and J. B. Hunter, "Prediction of vestibular schwannoma enlargement after radiosurgery using tumor shape and MRI texture features," *Otology & Neurotology*, vol. 42, no. 3, pp. E348–E354. 2021. https://doi.org/10.1097/MAO.0000000000002938

[12] Y. Itoyama, M. Matsuda, M. Suzuki, et al., "MRI radiomics-based prediction of vestibular schwannoma growth: a retrospective study," *European Archives of Oto-Rhino-Laryngology*, 2022. https://doi.org/10.1007/s00405-022-07479-4

[13] J. B. Patel, K. Vakharia, Y. Tao, et al., "Radiomics in head and neck cancer: basic principles and clinical applications," *Frontiers in Oncology*, 2022. — Vol. 12:851620. https://doi.org/10.3389/fonc.2022.851620

[14] S. Yüksel, A. Altunkeser, & E. Yıldız, "Vestibular Schwannoma with Superficial Siderosis: A Case Report," *Journal of Surgery and Medicine*, 4(11), 991–993, 2020. https://jsurgmed.com/article/download/649652/5578

[15] M. P. Strohl, & M. K. Wax, Symptoms, "Audiometric and Vestibular Laboratory Findings, and Imaging in a Concurrent Superior Canal Dehiscence Syndrome and Vestibular Schwannoma: A Case Report," *Journal of the American Academy of Audiology*, 31(6), 490–495, 2020. https://pubmed.ncbi.nlm.nih.gov/31267955/

[16] Jifeng Dai et al., Instance-sensitive Fully Convolutional Networks. 2016. eprint: [arXiv:1603.08678](https://arxiv.org/abs/1603.08678).

[17] Ronneberger Olaf, Fischer Philipp, and Brox Thomas. "U-Net: Convolutional Networks for Biomedical Image Segmentation," *LNCS*, vol. 9351, Oct. 2015, pp. 234–241. ISBN: 978-3-319-24573-7. https://doi.org/10.1007/978-3-319-24574-4_28.

[18] Kaiming He et al., "Mask R-CNN." *2017 IEEE International Conference on Computer Vision (ICCV),* 2017, pp. 2980–2988. https://doi.org/10.1109/ICCV.2017.322.

[19] Liang-Chieh Chen et al. "Encoder-Decoder with Atrous Separable Convolution for Semantic Image Segmentation," *Computer Vision – ECCV 2018: 15th European Conference*, Munich, Germany, September 8–14, 2018, Proceedings, Part VII, Springer-Verlag, 2018, pp. 833–851. ISBN: 978-3-030-01233-5. https://doi.org/10.1007/978-3-030-01234-2_49.

[20] Ze Liu et al., "Swin Transformer: Hierarchical Vision Transformer using Shifted Windows," 2021. arXiv: [2103.14030] (https://arxiv.org/abs/2103.14030).

[21] Zhenhong Sun et al., "Pyramid Attention Network for Semantic Segmentation," *BMVC*, 2018. URL: https://bmvc2018.org.

[22] Alexey Dosovitskiy et al., "An Image is Worth 16x16 Words: Transformers for Image Recognition at Scale," *International Conference on Learning Representations*, 2021. https://doi.org/10.48550/arXiv.2010.11929.

[23] Bichen Wu et al., "Visual Transformers: Token-based Image Representation and Processing for Computer Vision," *CoRR*, abs/2006.03677 (2020). https://doi.org/10.48550/arXiv.2006.03677.

[24] K. J. Park, S. C. Hwang, S. H. Park, D. H. Kang, J. Y Park, & J. H. Kim, "Hypervascular Vestibular Schwannoma: A Case Report," *Journal of the Korean Society of Radiology*, 71(5), 197–200, 2014. https://jksronline.org/DOIx.php?id=10.3348%2Fjksr.2014.71.5.197

[25] V. M. Ravindra, & W. T. Couldwell, "Vestibular Schwannoma of Oscillating Size: A Case Report and Review of the Literature," *Surgical Neurology International*, 3, 25, 2012. https://pmc.ncbi.nlm.nih.gov/articles/PMC3263002/

Received April 05, 2025

Sineglazov Victor. ORCID 0000-0002-3297-9060. Doctor of Engineering Science. Professor. Head of the Department Aviation Computer-Integrated Complexes.
Faculty of Air Navigation Electronics and Telecommunications, State University "Kyiv Aviation Institute", Kyiv, Ukraine.
Education: Kyiv Polytechnic Institute, Kyiv, Ukraine, (1973).
Research area: Air Navigation, Air Traffic Control, Identification of Complex Systems, Wind/Solar power plant, artificial intelligence.
Publications: more than 700 papers.
E-mail: svm@nau.edu.ua

Fedirko Volodymyr. ORCID 0000-0002-0411-6161. MD, PhD, DMSs.
Head of Subtentorial neurooncology department, Romodanov Institute of Neurosurgery NAMS of Ukraine, Kyiv, Ukraine.
Education: National Pirogov Memorial Medical University, Vinnytsya, (1985).
Research interests: neurooncology, hydrocephalus, hyperactive dysfunction syndrome of the cranial nerves, nerotrauma, craniobasal surgical approaches.
Publications: 181.
E-mail: fedirkovol@gmail.com

Shust Vasyl. ORCID 0000-0002-0459-9888. MD. PhD Student.
Subtentorial neurooncology department, Romodanov Institute of Neurosurgery NAMS of Ukraine, Kyiv, Ukraine.
Education: Bogomolets National Medical University, (2020).
Research interests: neurooncology, hydrocephalus, hyperactive dysfunction syndrome of the cranial nerves.
Publications: 6.
E-mail: vasulshust97@gmail.com

Sheruda Andrew. Master's degree
Department of Artificial Intelligence, Institute of Applied Systems Analysis, National Technical University of Ukraine "Igor Sikorsky Kyiv Polytechnic Institute", Kyiv, Ukraine.
Education: National Technical University of Ukraine "Igor Sikorsky Kyiv Polytechnic Institute", Kyiv, Ukraine, (2022).
Research interests: artificial neural networks, artificial intelligence, distributed computing.
Publications: 4.
E-mail: sheruda.andrew@lll.kpi.ua

Shevchenko Maksym. PhD student.
Aviation Computer-Integrated Complexes Department, Faculty of Air Navigation Electronics and Telecommunications, State University "Kyiv Aviation Institute", Kyiv, Ukraine.
Education: National Aviation University, Kyiv, Ukraine, (2020).

Research area: Identification of complex systems.
Publications: 2.
E-mail: maksymshevchenko01@gmail.com

В. М. Синєглазов, В. О. Федірко, В. В. Шуст, А. В. Шеруда, Шевченко М. В. Діагностика вестибулярної шванноми на основі інтелектуальної обробки зображень МРТ

У дослідженні було визначено основні клінічні та діагностичні особливості захворювання, розглянуто сучасні методи діагностики шванноми, зокрема магнітно-резонансну та комп'ютерну томографію, а також роль клінічного огляду, анамнезу та лабораторних аналізів, проаналізовано доступні відкриті дані та запропоновано концепцію поєднання медичних зображень з молекулярними індикаторами для побудови ефективніших діагностичних моделей на основі семантичної сегментації. Було узагальнено діагностичні та прогностичні біомаркери, включаючи TNF-α, CD68, CD163, IL-6, CCR2 та інші, що може підвищити точність прогнозування перебігу захворювання.

Ключові слова: вестибулярна шваннома; діагностичні та прогностичні біомаркери; МРТ-зображення; згорткова нейронна мережа; трансформатори; семантична сегментація.

Синєглазов Віктор Михайлович. ORCID 0000-0002-3297-9060. Доктор технічних наук. Професор. Завідувач кафедри авіаційних комп'ютерно-інтегрованих комплексів.
Факультет аеронавігації, електроніки і телекомунікацій, Державний університет «Київський авіаційний інститут», Київ, Україна.
Освіта: Київський політехнічний інститут, Київ, Україна, (1973).
Напрям наукової діяльності: аеронавігація, управління повітряним рухом, ідентифікація складних систем, вітроенергетичні установки, штучний інтелект.
Кількість публікацій: більше 700 наукових робіт.
E-mail: svm@nau.edu.ua

Федірко Володимир Олегович. ORCID 0000-0002-0411-6161. Лікар-нейрохірург. Доктор медичних наук.
Завідувач відділення субтенторіальної нейроонкології, ДУ «Інститут нейрохірургії ім. акад. А. П. Ромоданова НАМН України», Київ, Україна..
Освіта: Вінницький медичний інститут ім. М.І. Пирогова, (1985).
Напрям наукової діяльності: нейроонкологія, гідроцефалія, синдроми гіперактивної дисфункції черепних нервів, нейротравма, краніобазальні хірургічні доступи.
Кількість публікацій: 181.
E-mail: fedirkovol@gmail.com

Шуст Василь Володимирович. ORCID 0000-0002-0459-9888. Лікар-нейрохірург. Аспірант.
Відділення субтенторіальної нероонкології, ДУ «Інститут нейрохірургії ім. акад. А. П. Ромоданова НАМН України», Київ, Україна
Освіта: Національний медичний університет імені О. О. Богомольця, (2020).
Напрям наукової діяльності: нейроонкологія, гідроцефалія, синдроми гіперактивної дисфункції черепних нервів.
Кількість публікацій: 6
E-mail: vasulshust97@gmail.com

Шеруда Андрій Володимирович. Магістр.
Кафедра інформаційних систем, Факультет інформатики та обчислювальної техніки, Національний технічний університет України «Київський політехнічний інститут імені Ігоря Сікорського», Київ, Україна.
Освіта: Національний технічний університет Україні «Київський політехнічний інститут імені Ігоря Сікорського», (2022).
Напрям наукової діяльності: штучні нейронні мережі, штучний інтелект, розподіленні обчислення.
Кількість публікацій: 4.
E-mail: sheruda.andrew@lll.kpi.ua

Шевченко Максим Валерійович. Аспірант.
Кафедра авіаційних комп'ютерно-інтегрованих комплексів, Факультет аеронавігації, електроніки і телекомунікацій, Державний університет «Київський авіаційний інститут», Київ, Україна.
Освіта: Національний авіаційний університет, Київ, Україна, (2020).
Напрям наукової діяльності: ідентифікація складних систем.
Кількість публікацій: 2.
E-mail: maksymshevchenko01@gmail.com